biomolecules

MDPI

Article

Extracellular Vesicle-Mediated U1 snRNA Delivery Restores Aberrant Pre-mRNA Splicing in Human Cells

Hatice Esenkaya [1,2,*], Muhammet Karaman [3] and Joe Bryant [4]

[1] Department of Cell and Molecular Biology, Karolinska Institutet, 17 177 Stockholm, Sweden
[2] School of Life Sciences, Molecular Biology and Genetics, Kilis 7 Aralik University, 79000 Kilis, Turkey
[3] Department of Biology, Faculty of Science, Dokuz Eylul University, 35390 Izmir, Turkey
[4] School of Biosciences, Faculty of Health and Medical Sciences, University of Surrey, Guildford GU2 7XH, UK
* Correspondence: hatice.esenkaya@kilis.edu.tr or hatice.esenkaya@ki.se

Abstract

Splicing defects represent a significant class of human genetic disorders, yet strategies to directly correct aberrant splice-site recognition remain limited. The small nuclear RNA (snRNA) U1 plays a critical role in pre-messenger RNA splicing by base-pairing with the conserved 5′ splice-site 'GU' dinucleotide. Disruption of this interaction can lead to abnormal splicing or frameshift mutations, contributing to disease pathology. Extracellular vesicles (EVs) can transport small molecules to cells for therapeutic applications. Here, U1 snRNA-overexpressing HEK293T cells were used to generate approximately 120 nm-diameter U1 snRNA-enriched EVs, whose purity and content were confirmed by exosomal marker Western blots and reverse transcription–quantitative PCR. When HeLa cells expressing a β-globin minigene bearing a β-thalassaemia-like 5′ splice-site mutation were treated with U1-snRNA-enriched EVs, they corrected up to sixty percent of normal exon–intron junction recognition in a dose-dependent manner. Recovery was abolished by heat or RNase treatment, suggesting that intact vesicular RNA cargo was essential for activity. These findings provide the first demonstration that EVs can transport spliceosomal snRNAs capable of reconstituting splice-site recognition in recipient cells and introduce a novel class of RNA-based therapeutics that exploit the natural cargo-shuttling capacity of EVs to correct splicing defects associated with genetic disease.

Keywords: extracellular vesicles; U1 snRNA; RNA splicing; β-globin; splice-site mutation; RNA therapeutics; β-thalassaemia

Check for updates

Academic Editors: Ivan Poon and Paolo Ascenzi

Received: 12 December 2025
Revised: 27 January 2026
Accepted: 9 February 2026
Published: 10 February 2026

Copyright: © 2026 by the authors. Licensee MDPI, Basel, Switzerland. This article is an open access article distributed under the terms and conditions of the Creative Commons Attribution (CC BY) license.

1. Introduction

Precise and efficient pre-messenger RNA (pre-mRNA) splicing is essential for eukaryotic gene expression, ensuring that introns are accurately excised and exons correctly joined to form mature mRNA [1,2]. This process is catalysed by the spliceosome, a dynamic ribonucleoprotein complex composed of five small nuclear ribonucleoproteins (snRNPs), U1, U2, U4, U5, and U6, together with more than 300 auxiliary splicing factors [3,4]. The spliceosome, its role in alternative splicing, and human disease have been under investigation since the 1900s and have been covered frequently in recent reviews [5–7]. It has long been understood that among the snRNPs, U1 plays a pivotal role in the early stages of spliceosome assembly by recognising and base-pairing at the exon–intron boundary via the conserved 'GU' 5′ splice-site motif [8,9]. This recognition event defines the correct site for intron removal and is critical for maintaining the integrity of coding sequences.

Mutations that disrupt canonical 'GU' splice-site motifs or interfere with the U1 snRNA–5′ splice-site interaction are a major cause of inherited human diseases. More than 15% of all disease-associated mutations are predicted to affect RNA splicing, often resulting in exon skipping, intron retention, or the generation of aberrant transcripts [10,11]. Notably, single-nucleotide substitutions within the 5′ splice-site of the β-globin gene (HBB) pre-mRNA can impair or abolish U1 snRNP binding, which leads to abnormal pre-mRNA processing and a deficiency of functional β-globin chains, the hallmark of β-thalassaemia [12]. As of recently, therapies for dysfunctional splice sites in β-thalassaemia are still being developed [13], so there is still a gap in knowledge to find the optimal therapeutic method. Similar defective splice-site recognition mutations also contribute to the pathogenesis of diverse diseases [14], including neurodegenerative disorders [5,15,16], muscular dystrophies [17], and cancers [18–20]. So, a novel approach to treating defective 5′ splice-site recognition could possibly be applied extensively.

Therapeutic correction of splicing defects has traditionally relied on antisense oligonucleotides (ASOs), which are designed to modulate splice-site usage or exon inclusion, a topic that has been widely reviewed [20–23]. Some ASO-based therapies have proven clinically successful, such as nusinersen for spinal muscular atrophy [24,25], and there remains much hope for future ASO therapeutics [26]. However, issues remain, including dosage accuracy, toxicity [27], and targeted cellular uptake [28,29]. Therefore, an optimised delivery mechanism is essential to mitigate most of these problems [30,31]. Furthermore, ASOs act by steric hindrance, correcting downstream splicing outcomes, but do not fix the underlying genetic defect or restore the natural spliceosome-mediated recognition of splice-sites; hence, they treat the symptoms but not the cause, and therefore require continuous dosing [21,30,32]. In contrast, direct delivery of functional snRNAs offers the potential to reinstate normal splice-site pairing, thereby achieving a more physiological repair of pre-mRNA processing [33,34]. In fact, engineered U1 snRNAs have already shown promise in preclinical settings for various diseases [35–38]; however, delivery remains technically challenging as snRNAs must reach the nucleus and integrate with the complex endogenous snRNP machinery [39].

Many of these past U1-based therapeutic strategies have applied lentiviral vectors [36,39,40], which have been constantly improved in recent years but still must be specifically engineered and produced for transduction efficiency and specificity and run the risk of oncogenicity (due to off-target effects), toxicity, and immunogenicity (due to viral origin) [31,41,42]. On the other hand, extracellular vesicles (EVs) have emerged as promising vectors for RNA delivery owing to their endogenous origin, stability in biological fluids, and intrinsic capacity to transfer functional nucleic acids (mRNAs, microRNAs, and long non-coding RNAs) between cells [43–45]. EVs encompass a heterogeneous population of membrane-bound vesicles, including exosomes (30–150 nm) and microvesicles (100–1000 nm), which are released through distinct biogenesis pathways [44,46]. Membrane proteins that contribute to vesicle formation and cargo selection are enriched in exosomes, like the endosomal sorting complex protein TSG101 and Tetraspanins, including CD9, CD63, and CD81 [44,47]. Their natural capacity for targeted intracellular delivery has stimulated interest in exploiting EVs as therapeutic carriers for RNA-based interventions [45,46,48,49]. Indeed, recent studies have demonstrated that EVs have the potential to transfer functional RNA species capable of modulating gene expression, regulating translation, and altering cellular phenotypes [48,50]. They are typically less efficient than lentiviral vectors as their cargo is often episomal rather than integrating into the genome, but they are safer, with less oncogenicity and immunogenicity [51,52]. Despite the benefits of EVs as delivery vectors and U1 snRNA for splicing restoration, the use of EVs to deliver spliceosomal components such as U1 snRNA has not been previously reported.

The U1 snRNA has a relatively small, stable, and well-defined structure, making it an ideal candidate for encapsulation and intercellular delivery [39,53]. Hence, we investigated whether engineered EVs can carry U1 snRNA to recipient cells for intracellular uptake and reassembly into fully functional snRNP complexes in vitro in order to rescue defective 5′ splice-site recognition in target pre-mRNA substrates. In brief, U1 snRNA transcript-enriched EVs were generated by U1 snRNA-overexpressing HEK293T cells, isolated with differential ultracentrifugation and filtration, and then characterised with both nanoparticle tracking analysis (NTA) and canonical marker-based Western blotting. HeLa cells that mimic β-thalassaemia disease were then treated with these U1 snRNA-enriched EVs. By measuring stability, dose-dependence, and RNA dependency, our results demonstrate for the first time that EV-delivered U1 snRNA can reconstitute splice-site recognition and partially rescue normal β-globin pre-mRNA processing in recipient cells.

We introduce a new framework for using EVs as natural carriers for spliceosomal RNAs, thereby expanding the scope of possibilities for RNA-based therapeutics to include the direct restoration of pre-mRNA splicing fidelity. Beyond its proof-of-concept nature, this approach holds potential for future treatments, including for a broad range of genetic disorders arising from splice-site mutations, and sets the stage for future development of EV-mediated snRNA delivery platforms.

2. Materials and Methods

2.1. Cell Culture

HEK293T and HeLa cells were obtained from authenticated laboratory stocks and routinely confirmed to be mycoplasma-free. Cells were maintained in Dulbecco's Modified Eagle Medium (DMEM; Gibco, Thermo Fisher Scientific, Waltham, MA, USA) supplemented with 10% foetal bovine serum (FBS; Sigma-Aldrich, Darmstadt, Germany), 100 U/mL penicillin, and 100 µg/mL streptomycin. To prevent contamination of extracellular vesicle (EV) preparations with bovine-derived vesicles, FBS was pre-depleted of EVs by ultracentrifugation at 100,000× *g* for 16 h at 4 °C using a Beckman Coulter Type 45 Ti rotor. All cell cultures were maintained at 37 °C in a humidified incubator with 5% CO_2 and passaged using 0.05% trypsin–EDTA at 70–80% confluence. Experiments were conducted using cells at passages below 20 to ensure phenotypic stability. Of note, HeLa cells were used due to their non-erythroid nature, meaning there is an absence of endogenous β-globin expression, and β-globin RNAs detected in downstream analysis were exogenously introduced from the EVs that did not originate in the HeLa cells.

2.2. U1 snRNA Expression Cassette

A human U1 snRNA transcriptional cassette, including its native promoter, coding region, and 3′ regulatory elements, was synthesised (Integrated DNA Technologies, Collarville, IA, USA) and cloned into pcDNA3.1. The cassette was designed to preserve the endogenous U1 secondary structure required for spliceosomal assembly. HEK293T cells were transiently transfected with these modified pcDNA3.1 plasmid vectors using Lipofectamine 3000 (Thermo Fisher Scientific) following the manufacturer's instructions. This media with Lipofectamine was completely replaced after 6 h with low glucose media (OptiMEM). Empty pcDNA3.1 vectors served as negative controls. Resulting U1 snRNA-overexpressing HEK293T cells were collected for U1 snRNA-enriched EV isolation 48 h post-transfection.

2.3. Extracellular Vesicle Isolation

EVs were purified from HEK293T cells in the low glucose OptiMEM without a transfection reagent using differential ultracentrifugation. Conditioned medium was collected, centrifuged at 300× *g* for 10 min to remove cells, and then at 2000× *g* for 20 min to remove

debris, followed by centrifugation at 10,000× *g* for 30 min to eliminate large vesicles and apoptotic bodies. The resulting supernatant was filtered through a 0.22 µm filter and ultracentrifuged at 100,000× *g* for 70 min at 4 °C. Pellets were washed in PBS and ultracentrifuged again at 100,000× *g* for 70 min. Final EV pellets were resuspended in sterile PBS and stored at −80 °C for short-term use. All steps were performed at 4 °C. This method is according to MISEV2018 guidelines [44].

2.4. Nanoparticle Tracking Analysis (NTA)

EV size and concentration were measured using a NanoSight NS300 system (Malvern Instruments, Malvern, UK). EV preparations were diluted 1:100–1:500 in PBS to reach optimal particle concentrations (~1 × 10^8 particles/mL). For each sample, five 60 s videos were acquired with identical camera settings across 3 biological replicates. Data were processed using NTA NanoSight NS300 system (v3.4.4) software (version 67397) to calculate median diameter and span from the total particle yield concentrations in particles/mL, as well as particles recovered at peak size, which were displayed in Microsoft Excel (version 2601), where *t*-test statistics were calculated (Supplementary Data). Span was calculated as (D90 − D10)/D50, based on percentile diameters derived from the particle size distribution. This is a NanoSight-specific size distribution metric distinct from polydispersity index because its calculation does not assume a Gaussian distribution, which can be more appropriate for skewed particle populations, such as extracellular vesicles (Supplementary Data). NanoSight NS300 system settings were kept as similar between readings as possible: 24 °C, 100 shutter, 30 fps, and 80 camera sensitivity (Supplementary Data).

2.5. Western Blot Analysis of EV Markers

Three biological replicates of EVs and their corresponding donor cell lysates were lysed in RIPA buffer supplemented with protease inhibitors (Roche, Basel, Switzerland). Equal protein amounts from 3 biological replicates were resolved on SDS–PAGE gels and transferred to PVDF membranes. Membranes were probed with primary antibodies against CD9, CD63, TSG101 (canonical EV markers), and calnexin (negative control marker for endoplasmic reticulum contamination). Binding was visualised using HRP-conjugated secondary antibodies and enhanced chemiluminescence (ECL; GE Healthcare Chicago, IL, USA). Blots were quantified using ImageJ software (version v1.53c), and the sample of interest relative to control analysis was calculated and plotted in Microsoft Excel (Supplementary Data).

2.6. RNA Extraction from EVs

EV RNA was extracted using TRIzol LS reagent (Thermo Fisher Scientific) according to the manufacturer's protocol. Glycogen (Thermo Fisher Scientific) was used as a carrier to enhance yield. RNA quantity and purity were assessed via NanoDrop spectrophotometry (Thermo Fisher Scientific, Wilmington, DE, USA).

2.7. Construction of β-Globin Minigene Constructs

Human β-globin minigenes encompassing exons 1–3 and their intervening introns (~2.2 kb) were amplified from human genomic DNA and cloned into the pcDNA3.1(+) vector downstream of the CMV promoter using standard restriction–ligation cloning. The β-thalassaemia-like mutant vector construct was generated by introducing a G→A substitution at the +1 position of intron 2, disrupting the canonical 5′ splice-site 'GU' dinucleotide. Mutations were introduced using the QuikChange II Site-Directed Mutagenesis Kit (Agilent Technologies, Santa Clara, CA, USA) and confirmed by Sanger sequencing. Vector constructs were propagated in DH5α E. coli and purified using the EndoFree Plasmid Maxi Kit (Qiagen, Hilden, Germany) according to the manufacturer's instructions.

2.8. HeLa Cell Transfection with β-Globin Minigene Constructs

HeLa cells were seeded in 12-well plates at 1×10^5 cells per well in three biological replicates. After 24 h, cells were transfected with 500 ng of wild-type or mutant β-globin minigene vector constructs using Lipofectamine 3000. These cells were cultured for at least six hours post-transfection before further experimentation. Successful HeLa cell transformants with the minigene were designed to mimic β-thalassaemia.

2.9. β-Thalassaemia Mimic HeLa Cell Treatment with U1 snRNA-Enriched EVs

Either snRNA-enriched or control (empty) EVs were added directly to the culture medium without transfection agents. Cells were harvested 48 h after EV addition.

2.10. RT–PCR Splicing Analysis

Total RNA from HeLa cells was isolated using the RNeasy Mini Kit (Qiagen, Hilden, Germany) with kit on-column DNase I treatment. cDNA synthesis was performed with the High-Capacity cDNA Reverse Transcription Kit (Applied Biosystems, Waltham, MA, USA). β-Globin transcripts were amplified using reporter-specific primer sets located in exon 1 (forward) and exon 3 (reverse). PCR cycles were optimised to remain within the linear amplification range. Products were resolved on 2% agarose gels, visualised with ethidium bromide. Spliced and unspliced bands were gel-excised and sequenced for verification.

2.11. Quantitative RT–PCR

Isoform-specific qPCR assays were designed to detect either the correctly spliced transcript or the intron-retaining species. Reactions were performed with Power SYBR Green Master Mix (Applied Biosystems) on a QuantStudio 5 real-time PCR system. Spliced U1 gene expression was normalised to GAPDH or U6 snRNA, and then U1-containing EVs were shown relative to empty EVs. Fold changes were calculated using the $2^{-\Delta\Delta Ct}$ method in Microsoft Excel (Supplementary Data). All reactions were performed in triplicate.

2.12. Statistical Analysis

All experiments included at least two biological replicates. Data are presented as mean or median ± standard deviation (SD). Statistical analyses were performed using Microsoft Excel. One- or two-tailed Welch's *t*-tests were used for significance comparisons. *p*-values < 0.05 were considered statistically significant.

3. Results

3.1. Characterisation of U1 snRNA-Enriched Extracellular Vesicles

A U1 snRNA-overexpressing HEK293T cell line was generated to assess whether cells can be manipulated into packaging excess U1 snRNA transcripts into EVs to generate 'U1 snRNA-enriched' EVs for harvest and downstream applications. To achieve this, HEK293T cells were transfected with a pcDNA3.1 expression vector containing a U1 snRNA expression cassette or an empty vector as a control. Transfected cells were left for 6 h, and after 6 h, the condition media was changed to OptiMEM low glucose media for 48 h before EVs were isolated from the conditioned medium by sequential centrifugation, followed by filtration and ultracentrifugation (Figure 1A). Nanoparticle tracking analysis (NTA) of isolated EVs revealed a size distribution centred around 120 nm with spans typically between 0.75 and 1.1 (Supplementary Data). These are consistent with the expected exosomal range and have small variation between biological replicates, suggesting consistent preparation quality and particle heterogeneity during EV extractions (Figure 1B). There was no significant difference in the median size across all particles measured in U1 snRNA-enriched vs. either U2-containing EVs (p = 0.56), or the empty control (p = 0.45) (Figure 1C). Meanwhile,

the total particle yield from U1 snRNA-enriched EVs averaged 5.6 × 10^{12} particles per millilitre, again with no significant difference compared to total particles from cells treated with U2-enriched (p = 0.63) or empty control EVs (p = 0.39) (Figure 1D). Overall, there were 39% less total particles/mL from the cells treated with U1-enriched EVs than from cells treated with empty EV controls (Figure 1D). But at peak particle diameter, there were, on average, 54% more particles/mL in U1 snRNA-enriched EVs and 16% more particles/mL in U2-containing EVs compared to the empty EV controls (Figure 1E). This suggests a smaller overall yield of snRNA-containing EVs, but they are still suitable and very consistent.

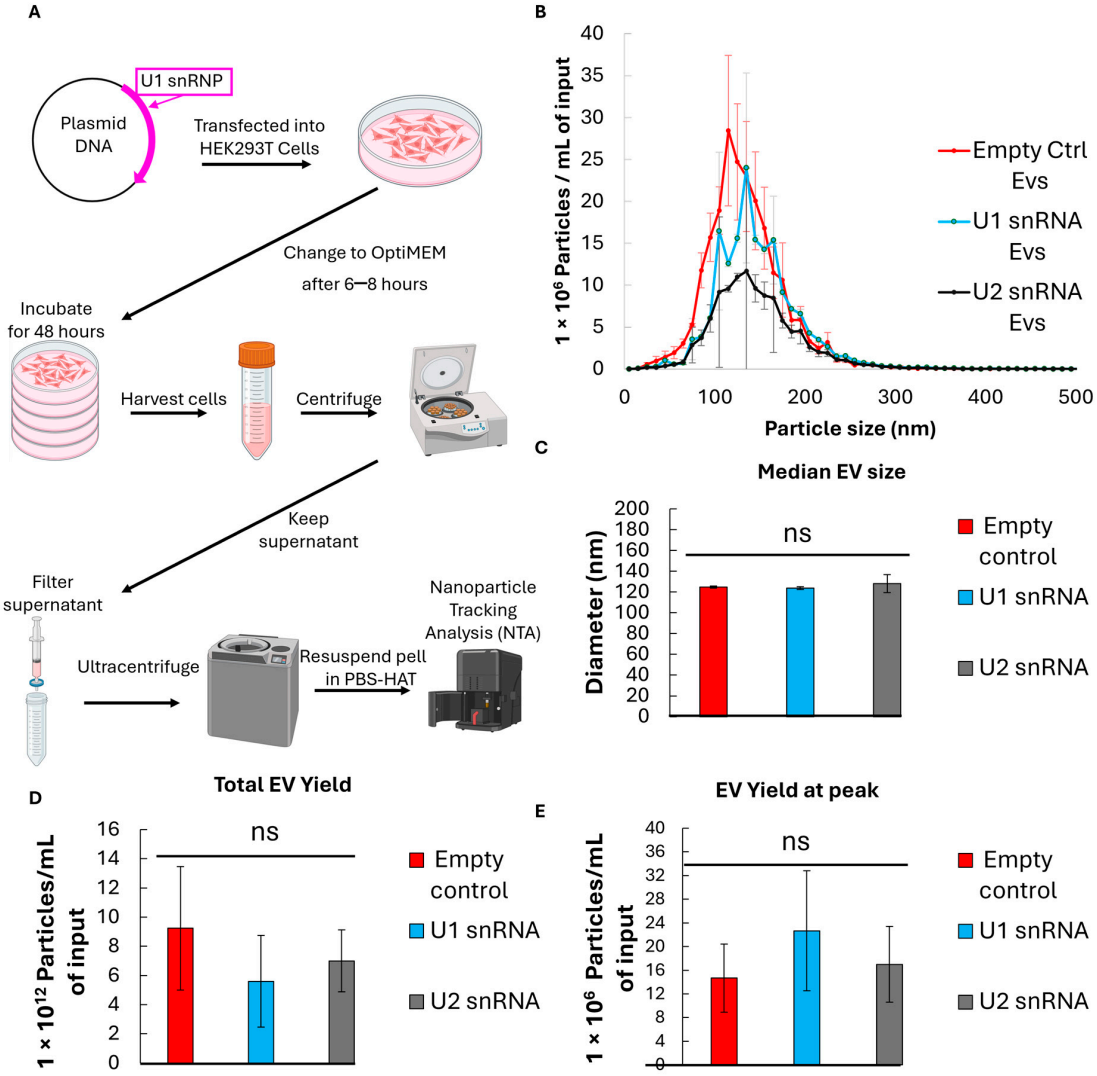


Figure 1. EV isolation and classification by nanoparticle tracking analysis (NTA). (**A**) Schematic representation of the NTA method. A native human U1 snRNP expression cassette was cloned into the pcDNA3.1 plasmid (**top left**). HEK293T cells were transfected with this vector and grown in OptiMEM for 6 h before replacement with OptiMEM low glucose (**middle left**). After 48 h, cells were collected by differential centrifugation (**middle right**). The supernatant was filtered through and ultracentrifuged to pellet EVs (**middle bottom**). Pellets were washed and resuspended in PBS, and the size and concentration were measured with a NanoSight NS300 system. (**B**) Size distribution analysis comparing U1 (light blue) and U2 (dark grey) snRNA-containing EVs to empty control EVs (red). Error bars represent standard deviation between 3 biological replicates (n = 3). (**C**–**E**) Total EV median diameter and average overall or peak size yields of isolated control EVs (red), U1-containing EVs (light blue), and U2-containing EVs (dark grey). Error bars show standard deviation between 3 biological replicates (n = 3). Significance values are calculated with a two-tailed Welch's t-test, and differences between all EV replicates were non-significant (ns) >0.3.

Western blot analysis confirmed the presence of canonical exosomal markers CD9, CD63, and TSG101, while cellular contaminants such as calnexin were undetectable, indicating high purity of the preparations (Figure 2). Together, these data confirm that U1-expressing donor cells produce bona fide exosome-like vesicles suitable for downstream delivery experiments.

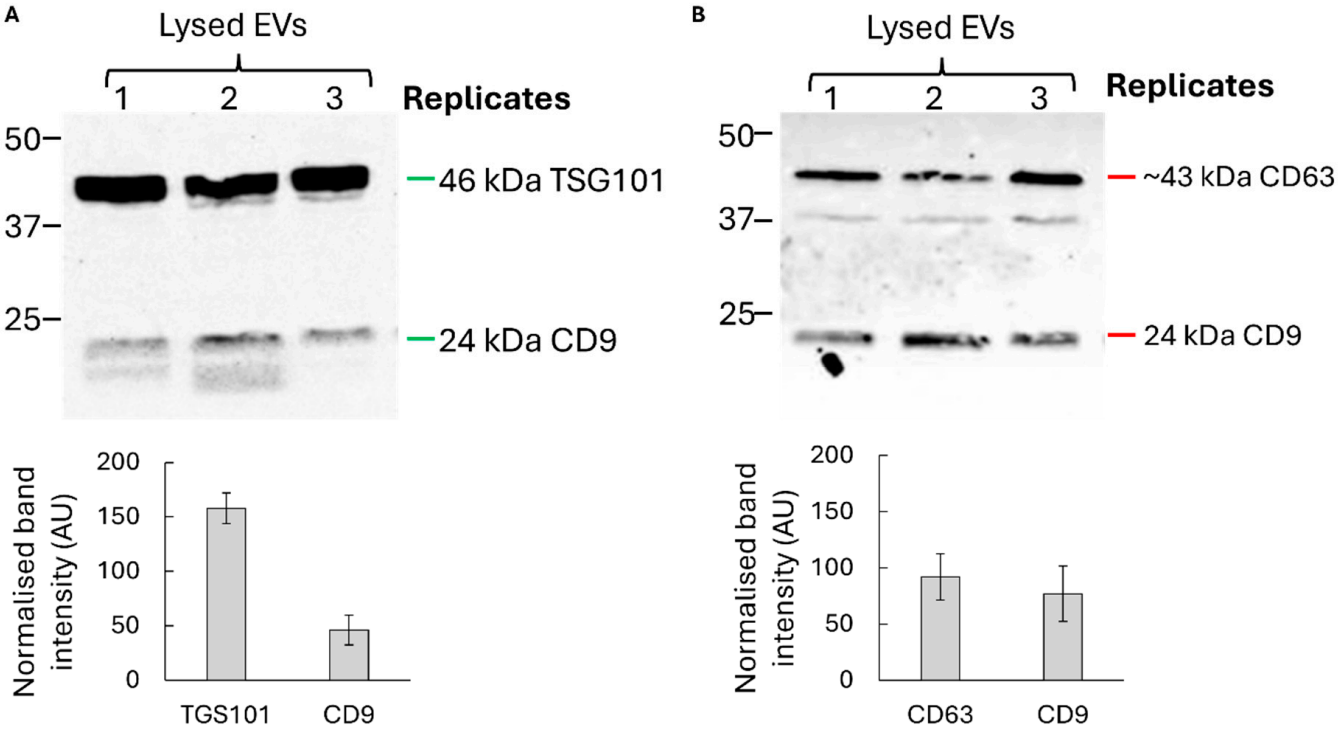


Figure 2. EV validation by Western blot analysis. (**A**,**B**) EV positive markers displayed in blots in biological triplicates (n = 3) and quantified below in bar graphs with error bars showing the standard deviation. (**A**) TSG101 and Cd9 markers; (**B**) CD63 and CD9. CD63 size is approximate and has two bands due to post-translational modifications. The original Western blot images are provided in the Supplementary Materials (Figure S3).

3.2. Detection of U1 snRNA Within Isolated EVs

To verify the successful loading of U1 snRNA into U1 snRNA-enriched EVs, total RNA was extracted from an equal number of vesicles isolated from control Hek293 cells (transfected with empty pcDNA3.1) or U1-overexpression Hek293 cells (transfected with the new pcDNA3.1 construct containing the U1 snRNA expression cassette). Reverse transcription followed by quantitative reverse transcriptase PCR (RT–qPCR) using U1-specific primers revealed a significant enrichment of U1 transcripts within EVs from U1-overexpressing cells ($p = 0.009$), compared to vector controls (Figure 3A). The relative U1 content was normalised to small RNA U6, which served as an internal reference.

The presence of U1 snRNA within U1 snRNA-enriched EVs was further validated by RNase protection assay. Treatment of intact U1 snRNA-enriched EVs with RNase A did not reduce the detectable U1 signal, whereas detergent-disrupted vesicles exhibited substantial degradation of U1 RNA (Figure 3B). This indicates that U1 snRNA is encapsulated within the vesicular lumen rather than externally associated with the vesicle surface. These findings collectively demonstrate that donor cell overexpression leads to efficient packaging of U1 snRNA into secreted EVs.

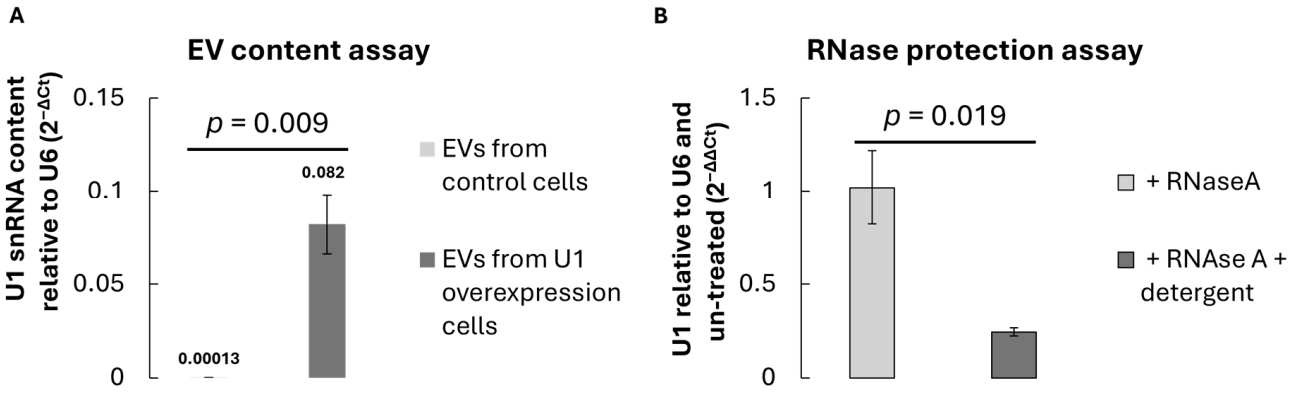


Figure 3. Identification and validation of U1 snRNA within EVs isolated from U1 overexpression HEK293 cells. (**A**) RT-qPCR highlights inclusion of U1 snRNA within EVs from control HEK293 cells (white) and EVs isolated from U1 overexpression cells (grey). Expression is relative to U6 snRNA reference and calculated with ($2^{-\Delta Ct}$). (**B**) RT-qPCR displaying U1 snRNA content from U1 overexpression HEK293 cells, relative to U6 snRNA and control cell-isolated EVs ($2^{-\Delta\Delta Ct}$), upon treatment with RNAseA only (grey) or RNAseA with detergent (dark grey). (**A**,**B**) Error bars show standard deviation between 3 biological replicates (n = 3). Significance is determined by one-tailed Welch's *t*-tests.

3.3. Restoration of β-Globin Pre-mRNA Splicing by U1-Containing EVs

To determine whether EV-delivered U1 snRNA can restore accurate pre-mRNA splicing, HeLa cells were transfected with a β-globin minigene construct bearing a β-thalassaemia-like 5′ splice-site mutation (G→A substitution at position +1). This mutation disrupts the canonical U1 snRNA binding site, resulting in aberrant splicing and the appearance of an intron-retained transcript, such as is found in β-thalassaemia (Figure 4A). β-thalassaemia-mimic HeLa cells were then treated with increasing concentrations of U1 snRNA-enriched EVs for 24 h. RT-PCR analysis of β-globin transcripts revealed a significant restoration of the correctly spliced mRNA isoform dependent on the dose (1×10^7 ($p = 0.096$), 1×10^8 ($p = 0.015$), or 1×10^9 ($p = 0.004$)), with up to 60% correction at the highest vesicle dose tested (Figure 4B). That represents 48% more splicing correction than background observed in cells treated with the empty control EVs lacking U1 RNA. Notably, this correction efficiency correlated with the amount of U1 expression in β-thalassaemia-mimic HeLa cells treated with U1-enriched EVs, which was measured by RT-qPCR (Figure 4C). This indicates a direct relationship between vesicular U1 content and splicing restoration.

To confirm that the observed rescue was mediated by intact RNA cargo, U1-enriched EVs were pre-treated with RNase or heat-inactivated before addition to cells. Both RNase and heat controls significantly reduced splicing recovery, even compared to 1×10^7 treatment ($p \leq 0.05$), and no longer showed significant differences to the empty EV control with $p = 0.28$ and $p = 0.12$, respectively. Therefore, the corrective effect was abolished, confirming that functional U1 RNA encapsulated within EVs is essential for restoring splicing fidelity (Figure 4D).

3.4. Functional Validation and Specificity of U1-Mediated Correction

To assess the specificity of U1-dependent splicing rescue, EVs enriched in unrelated small RNAs (U2 snRNA or miR-16) were prepared and applied to the mutant β-globin system. These alternative RNA-loaded vesicles restored significantly less normal splicing than 1×10^9 U1 snRNA ($p < 0.06$), underscoring the specificity of U1 snRNA for 5′ splice-site recognition (Figure 5).

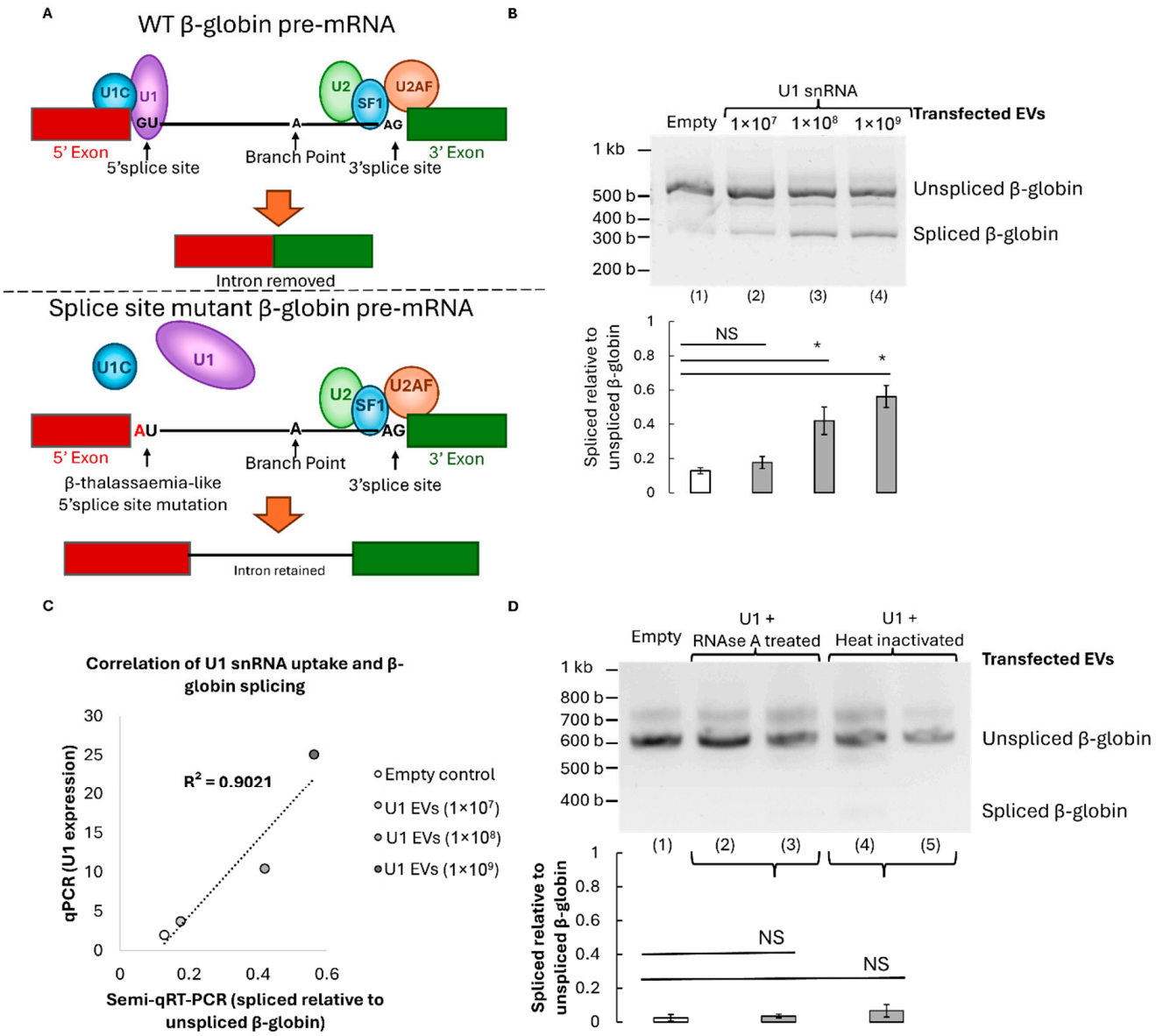


Figure 4. β-thalassemia-like β-globin pre-mRNA splicing can be rescued by U1-containing EVs. (**A**) Schematic representation of the splicing mechanism. Top shows a canonical representation of a section of the WT β-globin pre-mRNA consisting of a 5′ exon in red, an intron to be spliced out in black, and a second exon on the 3′ end in green. Several critical members of the spliceosome are shown, including U1 (purple), along with various auxiliary splicing factors. When the wild-type 'GU' dinucleotide is available, U1 (purple) base pairs are there to initiate splicing (**top**). Without this association, in the mutant β-globin system (**bottom**), U1 cannot bind, causing intron retention and dysfunctional β-globin production. The orange arrows show RNA products after splicing. (**B**) Representative RT-PCR displaying expression of spliced and unspliced β-globin pre-mRNA after treatment with empty EVs (1), or 1×10^7, 1×10^8, or 1×10^9 EVs containing U1 snRNA (2–4). Quantifications represent averages across two biological replicates (n = 2). (**C**) Plot displaying the correlation between U1 snRNA-containing EV amount and splicing recovery in mutant β-globin HeLa cells. (**D**) Representative RT-PCR (**top**) highlighting the expression of spliced or unspliced β-globin pre-mRNA isoforms in β-globin mutant cells treated with EVs containing an empty control (1), or U1 snRNAs (2–5). Prior to treatment, lane (2–3) technical replicates were RNAse-treated, while lane 4–5 technical replicates were heat-inactivated. Bands were quantified (**bottom**) in three biological replicates (n = 3), each with two technical replicates. Significance calculated with one-tailed Welch's *t*-tests; * $p \leq 0.05$; not significant (ns) $p \geq 0.05$. The original Western blot images are provided in the Supplementary Materials (Figures S4 and S5).

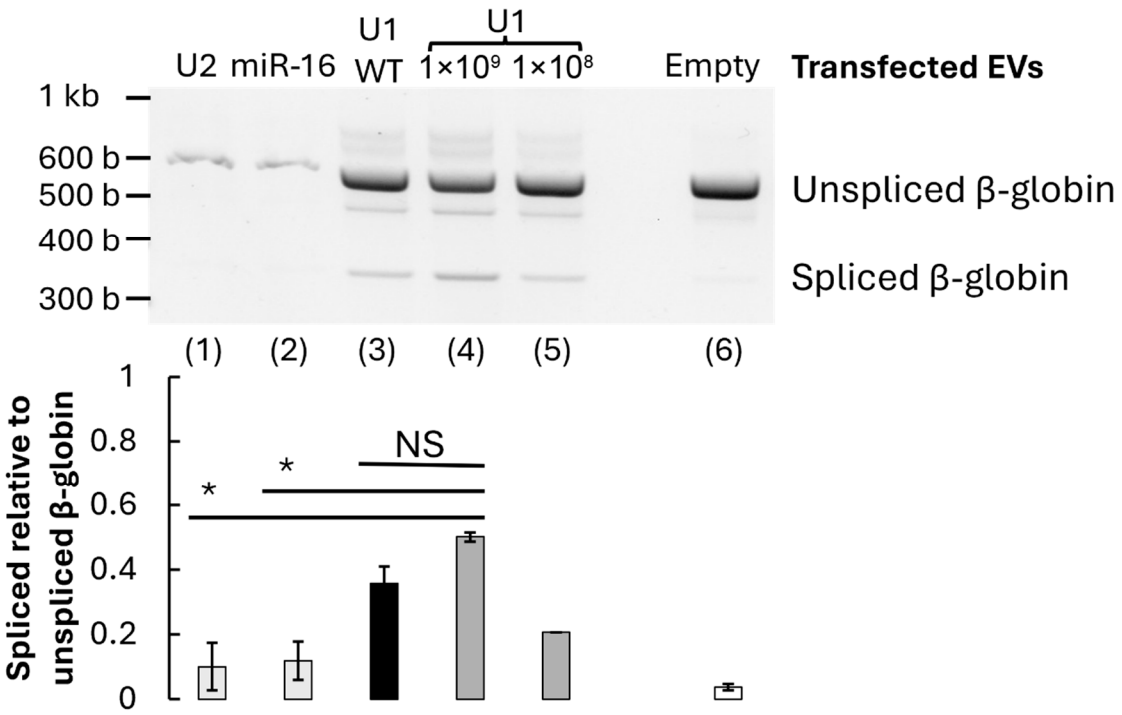


Figure 5. Validation of U1-mediated splicing recovery. RT-PCR expression example (**top**) and quantification (**bottom**) of spliced or unspliced β-globin pre-mRNA isoforms (n = 2–3). HeLa cells treated with EVs contained U2 snRNA control (1, light grey), miR-16 control (2, light grey), U1 snRNA (3, black), U1 snRNA at 1×10^9 or 1×10^8 concentrations (4/5, dark grey), or empty EV control (6, white). Mutant β-globin cells were treated with each RNA except the lane (3, black) control, where wild-type (WT) β-globin cells were treated with U1-enriched snRNA. Significance calculated with one-tailed Welch's *t*-tests; * $p \leq 0.05$; not significant (ns) $p \geq 0.05$. The original Western blot images are provided in the Supplementary Materials (Figure S6).

Furthermore, when wild-type β-globin reporter cells were treated with U1-enriched EVs, there was no substantial change in the WT splicing pattern or significant difference between the WT and mutant β-globin U1 1×10^9 treated cells ($p > 0.1$). This suggests that the treatment does not perturb normal splicing in unaffected contexts and brings splicing levels closer to WT levels (Figure 5).

Collectively, these results demonstrate that EV-mediated delivery of U1 snRNA specifically reconstitutes splice-site recognition in defective pre-mRNA and represents a targeted, functional correction of splicing defects in vitro.

4. Discussion

4.1. EVs as Vehicles for Functional RNA Transfer

Extracellular vesicles have emerged as powerful mediators of intercellular communication, capable of transferring proteins, lipids, and nucleic acids between cells [48,49]. Indeed, numerous studies have described EV-mediated transfer of most of the classes of rapidly evolving RNA-based drugs, including microRNAs, mRNAs, ASOs, and long non-coding RNAs that influence gene expression and cellular phenotype, which are being continuously expanded thanks in part to advances in structural analysis like nuclear magnetic resonance (NMR), which aids in the discovery of new small molecules [54,55]. The delivery of spliceosomal small nuclear RNAs has not previously been reported. We observed that U1-containing EVs maintain the typical size and marker profile of exosomes, indicating that snRNA loading does not disrupt vesicle biogenesis. This suggests that small nuclear RNAs may follow similar loading pathways to other small RNAs, possibly

involving RNA-binding proteins such as hnRNPA2B1 [56] or SYNCRIP [57], which have been implicated in the selective enrichment of RNA motifs within EVs.

Our method does not presume to include snRNAs as a therapeutic but demonstrates, as a proof-of-concept, that U1 snRNA can be selectively incorporated into EVs upon donor cell overexpression and that these vesicles retain the molecular integrity and activity of the RNA cargo. This is certainly an important first step because one of the largest remaining drawbacks of RNA therapeutics is the delivery mechanism, including delivery, durability, manufacturability, and safety/immune activation [54], which EVs can improve when compared to other viral or non-viral vectors. The pros and cons of each vector and their recent developments are extensively reviewed [58,59]. However, extracellular vesicles are often overlooked due to large-scale production difficulties [60], despite offering several intrinsic advantages for in vivo delivery. They are stable in circulation and can be modified for tissue-specific targeting, even across the blood–brain barrier, which other vectors struggle with [61]. Moreover, because EVs originate from endogenous membranes, they are less likely to induce adverse immune reactions compared with synthetic nanoparticles [49]. Hence, the ability to load and deliver small, structured RNAs, such as U1, through EVs opens possibilities for designing precision RNA therapeutics that restore splice-site recognition in affected tissues.

4.2. Considerations for U1-Mediated Splicing Rescue

The correction of β-globin splicing defects by U1-enriched EVs suggests that vesicle-delivered U1 RNA is not only internalised but remains functional after transfer and incorporates into the recipient cell's spliceosomal machinery, engaging directly with pre-mRNA substrates. These findings imply that EV-mediated RNA transfer can extend beyond regulatory microRNAs to include core components of the splicing machinery itself. However, the precise intracellular fate of the transferred RNA remains to be elucidated. Despite this, several possibilities can be considered. After uptake via endocytosis, vesicles may release their cargo into the cytoplasm [62], from where U1 snRNA could enter the nucleus through the canonical importin-mediated pathway used by endogenous snRNPs [63]. Alternatively, EVs might fuse with the plasma membrane or endosomal compartments to directly release their contents into the nucleocytoplasmic space [64]. To answer these questions, EVs could be engineered with fluorescent membrane reporters with palmitoylation signals and U1 snRNAs tagged with fluorescent aptamers to visualise the intracellular progression of the EVs and activity of U1 snRNA [65]. This would also be a great step toward elucidating the mechanism by which our method restores splicing. The observed dependence on intact RNA cargo—as shown by the loss of function after RNase or heat treatment—confirms that the restorative effect arises from genuine RNA activity rather than co-transferred proteins or secondary signals such as nucleic acid contamination, which would otherwise persist in these controls. To further improve clarity in the future, Northern blot analysis could also be included to visualise the purity and size of the RNA extracted from the U1-snRNA-enriched EVs.

The absence of off-target effects on wild-type splicing indicates that U1-mediated correction is both sequence-specific and context-dependent, which is consistent with the well-characterised base-pairing interaction between the 5′ end of U1 snRNA and the mutated donor splice-site sequence. Here, only wild-type U1 snRNA was applied to cells; however, previous studies have applied engineered U1 snRNAs to improve splicing. In these cases, the sequence of U1 snRNA was adapted to increase its complementarity specifically to the mutated splice-site donor [35,40]. This offers the possibility of further increasing the efficiency of splice-site correction in the future, possibly to achieve more than the 60% restoration identified here, which may be necessary if applying the treatment

in vivo. Indeed, chemical modifications to RNAs are currently under the spotlight due to their ability to enhance the stability of RNA, allowing for extended circulation time without restricting translation efficiency, even increasing protein production [66]. However, our preliminary method with unedited U1-snRNA within EVs is beneficial in its simplicity and in displaying the first use of naturally derived U1 snRNA to improve splicing efficiency. Although the β-globin mutant used in this study lacks a canonical GU 5′ splice site, rescue by wild-type U1 snRNA does not imply restoration of canonical splice-site recognition. Rather, U1 may support splicing through non-canonical mechanisms, including partial base-pairing, activation of cryptic donor sites, or indirect stabilisation of early spliceosome assembly. The precise molecular basis of this rescue remains to be determined.

4.3. Comparison with Existing RNA Therapeutic Approaches

Current molecular strategies for correcting splicing defects include antisense oligonucleotides (ASOs), small molecules, and gene-editing techniques. While ASOs have achieved clinical translation, particularly for disorders such as spinal muscular atrophy and Duchenne muscular dystrophy, they rely on repeated administration and often exhibit limited tissue penetration [29]. In contrast, EV-based delivery offers a naturally biocompatible and potentially self-targeting system with prolonged bioavailability. Unlike ASOs, which modulate splicing by steric blocking, U1 snRNA acts through restoration of native spliceosome recognition, thereby reinstating physiological processing of pre-mRNA [34,67]. Our findings thus highlight an important conceptual distinction: whereas ASOs compensate for defective splicing by redirecting the spliceosome, EV-delivered U1 directly reconstitutes a missing component of the splicing machinery. This approach could, in principle, complement or even surpass antisense therapies in specific contexts, particularly where the primary defect lies in impaired snRNA–splice-site pairing rather than regulatory mis-splicing. It is worth noting that these therapies have been suggested to improve efficacy when used in tandem, whereby ASO delivery can block intron retention while U1 delivery can reconstitute correct splicing [36]. Therefore, in more complicated splicing-related diseases, EV's could be used to deliver both ASOs and snRNAs.

5. Future Perspectives

Three doses were tested here, 1×10^7, 1×10^8, and 1×10^9, which are in line with clinical EV dosages, for example, those used in recent COVID-19 trials using: 5×10^7 [68], 2×10^8 [69], and 1×10^8–1×10^{10} [70], respectively, which have also been reviewed in [52]. At 1×10^9, we found a 60% improvement in splicing efficiency in vitro, which is a very solid starting point for our investigations. It is hard to directly compare this to clinical studies, as they report on clinical outcomes rather than the percentage of splicing recovery; however, even minor improvements in splicing restoration have been linked to meaningful outcomes. For example, a single low dose of nusinersen in children was found to have beneficial outcomes [71], and thus, when full-length copy numbers are as low as 10–15% initially [72], even small improvements can be biologically beneficial [73]. Regarding β-thalassaemia, mutations that completely abolish β-globin production (β^0) are associated with severe anaemia, whereas mutations permitting residual β-globin synthesis (β^+) are associated with milder phenotypes [74], again suggesting that even a small improvement in splicing would be biologically relevant.

Although this research offers exciting potential for the use of EVs to treat many monogenic disorders and tissue-specific genetic disorders in humans caused by splice-site mutations, our experiments were only performed in cultured HeLa cells using a model β-globin system. It would be interesting to expand to other cell lines or in vivo systems like β-thalassemia mouse models. However, many other fundamental questions

require answers, and optimisations must be made before therapeutics with U1 snRNA EVs could be considered. For example, to improve EV encapsulation efficiency, future studies could aim to identify RNA–protein interactions that govern U1 packaging and engineering of RNA-binding protein carriers [48,75]. U1 snRNA overexpression followed by immunoprecipitation, mass spectrometry, and RNA sequencing could identify binding partners, binding motifs, and sequence elements or secondary structures in the U1 snRNA important in U1 snRNA encapsulation [76]. This information could enable rational design of snRNA motifs, or co-overexpression of factors that initiate encapsulation, to enhance loading and enable up-scaled EV production. Alternatively, overexpression systems as used here can improve EV encapsulation [75]. Secondly, how can dosage efficiency be improved? Typically, they can be improved through the use of hydrogels for slow release [77,78]. Finally, to enable in vivo clinical applications, EV's also require engineering for targeting precision, and so how can EVs be targeted to specific cells if used in vivo? This has previously been done by the inclusion of antibodies or peptides on the EV surface [61,79], so it could be applied to snRNA delivery too. Another way to improve efficiency would be to introduce a sorting system to filter out any EVs that did not contain a suitably enriched U1 snRNA. Our approach has shown with RT-qPCR that the RNA is enriched overall compared to empty EVs, but we cannot establish what percentage of these EVs from U1-snRNA-overexpressing HEK293T cells are enriched. One possibility is that a fluorescent aptamer could be co-expressed with the snRNA to enable sorting with nano-flow cytometry, although sorting efficiency ($\leq$45%) and EV recovery ($\leq$10%) are typically low due to the small molecules being difficult to distinguish from background noise [80]. On the other hand, there are opportunities to use EV surface proteins in snRNA-enriched EVs for isolation before application to improve purity and dosage efficiency. Engineered CD63 is a common protein previously applied in such cases [81,82], so it could be applied to expand our methodology.

Finally, beyond U1, this platform could be extended to other snRNAs, small nucleolar RNAs (snoRNAs), or engineered RNA molecules designed to correct or modulate pre-mRNA processing. Such approaches might ultimately yield a new class of RNA therapeutics that operate at the level of the spliceosome itself.

6. Conclusions

The present study provides the first experimental evidence that naturally derived extracellular vesicles (EVs) can mediate the intercellular transfer of spliceosomal small nuclear RNAs and restore defective pre-mRNA splicing in human cells. Using a β-globin minigene model harbouring a β-thalassaemia-like 5′ splice-site mutation, we demonstrate that donor cells overexpressing U1 snRNA encapsulate functional U1 molecules, which, when delivered via engineered EVs, are capable of re-establishing canonical splice-site recognition. This finding expands the known functional repertoire of EV cargo and introduces a new RNA-based strategy for the correction of splicing-related genetic disorders, including β-thalassaemia, a range of neurodegenerative and muscular disorders, and cancers. Current challenges of applying EVs in therapeutics include loading, targeting, and dosage efficiencies; so future work will need to investigate scalable EV production systems, improved RNA loading strategies, and tissue-specific targeting methods in vivo.

Supplementary Materials: The following supporting information can be downloaded at: https://www.mdpi.com/article/10.3390/biom16020278/s1. File S1: Supplementary Data. Figure S1: qPCR data showing HeLa cell expression of U1 after EV transfections. Figure S2: NTA analysis stills. Figure S3: EV validation by Western blot analysis. Figure S4: Full RT-PCR gels displaying expression of spliced and unspliced β-globin pre-mRNA after transfection with empty EVs, or 1 × 107, 1 × 108 or 1 × 109 EVs containing U1 snRNA. Figure S5: Full RT-PCR gels highlighting the expression of

spliced or unspliced β-globin pre-mRNA isoforms in β-globin mutant cells transfected with EVs containing an empty control, or U1 snRNAs. Prior to transfection technical replicates were RNAse treated or heat inactivated. Figure S6: RT-PCR expression full gels showing spliced or unspliced β-globin pre-mRNA isoforms (n = 2–3).

Author Contributions: Conceptualisation, H.E. and M.K.; methodology, H.E. and M.K.; software, H.E. and J.B.; validation, H.E., M.K. and J.B.; formal analysis, H.E.; investigation, H.E. and M.K.; resources, H.E. and M.K.; data curation, H.E. and J.B.; writing—original draft preparation, H.E.; writing—review and editing, H.E. and J.B.; visualisation, H.E. and J.B.; project administration, H.E. All authors have read and agreed to the published version of the manuscript.

Funding: This research received no external funding.

Institutional Review Board Statement: Not applicable.

Informed Consent Statement: Not applicable.

Data Availability Statement: The original contributions presented in this study are included in the article/Supplementary Material. Further inquiries can be directed to the corresponding author.

Acknowledgments: BioRender software 201 was used to create the graphical abstracts and schematics in Figures 1A and 4A.

Conflicts of Interest: The authors declare no conflicts of interest.

References

1. Pan, Q.; Shai, O.; Lee, L.J.; Frey, B.J.; Blencowe, B.J. Deep surveying of alternative splicing complexity in the human transcriptome by high-throughput sequencing. *Nat. Genet.* **2008**, *40*, 1413–1415. [CrossRef]
2. Sakharkar, M.K.; Chow, V.T.K.; Kangueane, P. Distributions of exons and introns in the human genome. *In Silico Biol.* **2004**, *4*, 387–393. [CrossRef]
3. Zhang, X.; Yan, C.; Hang, J.; Finci, L.I.; Lei, J.; Shi, Y. An Atomic Structure of the Human Spliceosome. *Cell* **2017**, *169*, 918–929.e14. [CrossRef] [PubMed]
4. Pokorná, P.; Aupič, J.; Fica, S.M.; Magistrato, A. Decoding Spliceosome Dynamics through Computation and Experiment. *Chem. Rev.* **2025**, *125*, 9807–9833. [CrossRef]
5. Deutsch, H.M.; Song, Y.; Li, D. Spliceosome complex and neurodevelopmental disorders. *Curr. Opin. Genet. Dev.* **2025**, *93*, 102358. [CrossRef]
6. Pasteris, M.; Cakir, S.; Bellizzi, A.; Sariyer, I.K. Alternative splicing in Alzheimer's disease: Mechanisms, therapeutic implications, and 3D modeling approaches. *J. Alzheimer's Dis.* **2025**, *107*, 5–14. [CrossRef]
7. Soares, E.S.; Leal, C.B.Q.S.; Sinatti, V.V.C.; Bottós, R.M.; Zimmer, C.G.M. Role of the U1 snRNP Complex in Human Health and Disease. *WIREs RNA* **2025**, *16*, e70026. [CrossRef]
8. Furlong, R. Refining the splice region. *Nat. Rev. Genet.* **2018**, *19*, 470–471. [CrossRef] [PubMed]
9. Lerner, M.R.; Boyle, J.A.; Mount, S.M.; Wolin, S.L.; Steitz, J.A. Are snRNPs involved in splicing? *Nature* **1980**, *283*, 220–224. [CrossRef] [PubMed]
10. Krawczak, M.; Reiss, J.; Cooper, D. The mutational spectrum of single base-pair substitutions in mRNA splice junctions of human genes: Causes and consequences. *Hum. Genet.* **1992**, *90*, 41–54. [CrossRef]
11. Krawczak, M.; Thomas, N.S.; Hundrieser, B.; Mort, M.; Wittig, M.; Hampe, J.; Cooper, D.N. Single base-pair substitutions in exon-intron junctions of human genes: Nature, distribution, and consequences for mRNA splicing. *Hum. Mutat.* **2007**, *28*, 150–158. [CrossRef] [PubMed]
12. Treisman, R.; Orkin, S.H.; Maniatis, T. Specific transcription and RNA splicing defects in five cloned β-thalassaemia genes. *Nature* **1983**, *302*, 591–596. [CrossRef]
13. Lu, D.; Gong, X.; Guo, X.; Cai, Q.; Chen, Y.; Zhu, Y.; Sang, X.; Yang, H.; Xu, M.; Zeng, Y.; et al. Gene Editing of the Endogenous Cryptic 3′ Splice Site Corrects the RNA Splicing Defect in the β-Thalassemia Mouse Model. *Hum. Gene Ther.* **2024**, *35*, 825–837. [CrossRef]
14. Scotti, M.M.; Swanson, M.S. RNA mis-splicing in disease. *Nat. Rev. Genet.* **2016**, *17*, 19–32. [CrossRef]
15. Nava, C.; Cogne, B.; Santini, A.; Leitão, E.; Lecoquierre, F.; Chen, Y.; Stenton, S.L.; Besnard, T.; Heide, S.; Baer, S.; et al. Dominant variants in major spliceosome U4 and U5 small nuclear RNA genes cause neurodevelopmental disorders through splicing disruption. *Nat. Genet.* **2025**, *57*, 1374–1388. [CrossRef]
16. Nik, S.; Bowman, T.V. Splicing and neurodegeneration: Insights and mechanisms. *WIREs RNA* **2019**, *10*, e1532. [CrossRef]

17. Ottesen, E.W.; Singh, N.N.; Seo, J.; Singh, R.N. U1 snRNA interactions with deep intronic sequences regulate splicing of multiple exons of spinal muscular atrophy genes. *Front. Neurosci.* **2024**, *18*, 1412893. [CrossRef]
18. Urbanski, L.M.; Leclair, N.; Anczuków, O. Alternative-splicing defects in cancer: Splicing regulators and their downstream targets, guiding the way to novel cancer therapeutics. *WIREs RNA* **2018**, *9*, e1476. [CrossRef] [PubMed]
19. Bradley, R.K.; Anczuków, O. RNA splicing dysregulation and the hallmarks of cancer. *Nat. Rev. Cancer* **2023**, *23*, 135–155. [CrossRef]
20. Lv, X.; Sun, X.; Gao, Y.; Song, X.; Hu, X.; Gong, L.; Han, L.; He, M.; Wei, M. Targeting RNA splicing modulation: New perspectives for anticancer strategy? *J. Exp. Clin. Cancer Res.* **2025**, *44*, 32. [CrossRef] [PubMed]
21. Havens, M.A.; Hastings, M.L. Splice-switching antisense oligonucleotides as therapeutic drugs. *Nucleic Acids Res.* **2016**, *44*, 6549–6563. [CrossRef] [PubMed]
22. Wai, H.A.; Svobodova, E.; Herrera, N.R.; Douglas, A.G.L.; Holloway, J.W.; Baralle, F.E.; Baralle, M.; Baralle, D. Tailored antisense oligonucleotides designed to correct aberrant splicing reveal actionable groups of mutations for rare genetic disorders. *Exp. Mol. Med.* **2024**, *56*, 1816–1825. [CrossRef] [PubMed]
23. Chen, S.; Heendeniya, S.N.; Le, B.T.; Rahimizadeh, K.; Rabiee, N.; Zahra, Q.U.A.; Veedu, R.N. Splice-Modulating Antisense Oligonucleotides as Therapeutics for Inherited Metabolic Diseases. *BioDrugs* **2024**, *38*, 177–203. [CrossRef]
24. Finkel, R.S.; Mercuri, E.; Darras, B.T.; Connolly, A.M.; Kuntz, N.L.; Kirschner, J.; Chiriboga, C.A.; Saito, K.; Servais, L.; Tizzano, E.; et al. Nusinersen versus Sham Control in Infantile-Onset Spinal Muscular Atrophy. *N. Engl. J. Med.* **2017**, *377*, 1723–1732. [CrossRef]
25. Cebulla, G.; Hai, L.; Warnken, U.; Güngör, C.; Hoffmann, D.C.; Korporal-Kuhnke, M.; Wildemann, B.; Wick, W.; Kessler, T.; Weiler, M. Long-term CSF responses in adult patients with spinal muscular atrophy type 2 or 3 on treatment with nusinersen. *J. Neurol.* **2025**, *272*, 270. [CrossRef]
26. Wijnant, K.N.; Nadif Kasri, N.; Vissers, L.E. Systematic analysis of genetic and phenotypic characteristics reveals antisense oligonucleotide therapy potential for one-third of neurodevelopmental disorders. *Genome Med.* **2025**, *17*, 59. [CrossRef] [PubMed]
27. Sabrina Haque, U.; Kohut, M.; Yokota, T. Comprehensive review of adverse reactions and toxicology in ASO-based therapies for Duchenne Muscular Dystrophy: From FDA-approved drugs to peptide-conjugated ASO. *Curr. Res. Toxicol.* **2024**, *7*, 100182. [CrossRef]
28. Raguraman, P.; Balachandran, A.A.; Chen, S.; Diermeier, S.D.; Veedu, R.N. Antisense Oligonucleotide-Mediated Splice Switching: Potential Therapeutic Approach for Cancer Mitigation. *Cancers* **2021**, *13*, 5555. [CrossRef]
29. Gagliardi, M.; Ashizawa, A.T. The Challenges and Strategies of Antisense Oligonucleotide Drug Delivery. *Biomedicines* **2021**, *9*, 433. [CrossRef]
30. Lauffer, M.C.; van Roon-Mom, W.; Aartsma-Rus, A. Possibilities and limitations of antisense oligonucleotide therapies for the treatment of monogenic disorders. *Commun. Med.* **2024**, *4*, 6. [CrossRef]
31. Hammond, S.M.; Aartsma-Rus, A.; Alves, S.; Borgos, S.E.; Buijsen, R.A.M.; Collin, R.W.J.; Covello, G.; Denti, M.A.; Desviat, L.R.; Echevarría, L.; et al. Delivery of oligonucleotide-based therapeutics: Challenges and opportunities. *EMBO Mol. Med.* **2021**, *13*, e13243. [CrossRef] [PubMed]
32. Qiu, J.; Wu, L.; Qu, R.; Jiang, T.; Bai, J.; Sheng, L.; Feng, P.; Sun, J. History of development of the life-saving drug "Nusinersen" in spinal muscular atrophy. *Front. Cell. Neurosci.* **2022**, *16*, 942976. [CrossRef] [PubMed]
33. Zhuang, Y.; Weiner, A.M. A compensatory base change in U1 snRNA suppresses a 5′ splice site mutation. *Cell* **1986**, *46*, 827–835. [CrossRef]
34. Hatch, S.T.; Smargon, A.A.; Yeo, G.W. Engineered U1 snRNAs to modulate alternatively spliced exons. *Methods* **2022**, *205*, 140–148. [CrossRef]
35. Fernandez Alanis, E.; Pinotti, M.; Dal Mas, A.; Balestra, D.; Cavallari, N.; Rogalska, M.E.; Bernardi, F.; Pagani, F. An exon-specific U1 small nuclear RNA (snRNA) strategy to correct splicing defects. *Hum. Mol. Genet.* **2012**, *21*, 2389–2398. [CrossRef] [PubMed]
36. Breuel, S.; Vorm, M.; Bräuer, A.U.; Owczarek-Lipska, M.; Neidhardt, J. Combining Engineered U1 snRNA and Antisense Oligonucleotides to Improve the Treatment of a BBS1 Splice Site Mutation. *Mol. Ther. Nucleic Acids* **2019**, *18*, 123–130. [CrossRef]
37. Peruzzo, P.; Bergamin, N.; Bon, M.; Cappelli, S.; Longo, A.; Goina, E.; Stuani, C.; Buratti, E.; Dardis, A. Rescue of common and rare exon 2 skipping variants of the GAA gene using modified U1 snRNA. *Mol. Med.* **2025**, *31*, 45. [CrossRef]
38. Sönmezler, E.; Stuani, C.; Hız Kurul, S.; Güngör, S.; Buratti, E.; Oktay, Y. Characterization and Engineered U1 snRNA Rescue of Splicing Variants in a Turkish Neurodevelopmental Disease Cohort. *Hum. Mutat.* **2024**, *2024*, 7760556. [CrossRef]
39. Gonçalves, M.; Santos, J.I.; Coutinho, M.F.; Matos, L.; Alves, S. Development of Engineered-U1 snRNA Therapies: Current Status. *Int. J. Mol. Sci.* **2023**, *24*, 14617. [CrossRef]
40. Schmid, F.; Glaus, E.; Barthelmes, D.; Fliegauf, M.; Gaspar, H.; Nürnberg, G.; Nürnberg, P.; Omran, H.; Berger, W.; Neidhardt, J. U1 snRNA-mediated gene therapeutic correction of splice defects caused by an exceptionally mild BBS mutation. *Hum. Mutat.* **2011**, *32*, 815–824. [CrossRef]
41. Milone, M.C.; O'Doherty, U. Clinical use of lentiviral vectors. *Leukemia* **2018**, *32*, 1529–1541. [CrossRef]

42. Dong, W.; Kantor, B. Lentiviral Vectors for Delivery of Gene-Editing Systems Based on CRISPR/Cas: Current State and Perspectives. *Viruses* **2021**, *13*, 1288. [CrossRef]
43. Valadi, H.; Ekström, K.; Bossios, A.; Sjöstrand, M.; Lee, J.J.; Lötvall, J.O. Exosome-mediated transfer of mRNAs and microRNAs is a novel mechanism of genetic exchange between cells. *Nat. Cell Biol.* **2007**, *9*, 654–659. [CrossRef]
44. Théry, C.; Witwer, K.W.; Aikawa, E.; Alcaraz, M.J.; Anderson, J.D.; Andriantsitohaina, R.; Antoniou, A.; Arab, T.; Archer, F.; Atkin-Smith, G.K.; et al. Minimal information for studies of extracellular vesicles 2018 (MISEV2018): A position statement of the International Society for Extracellular Vesicles and update of the MISEV2014 guidelines. *J. Extracell. Vesicles* **2018**, *7*, 1535750. [CrossRef]
45. Kalluri, R.; LeBleu, V.S. The biology, function, and biomedical applications of exosomes. *Science* **2020**, *367*, eaau6977. [CrossRef]
46. El Andaloussi, S.; Mäger, I.; Breakefield, X.O.; Wood, M.J.A. Extracellular vesicles: Biology and emerging therapeutic opportunities. *Nat. Rev. Drug Discov.* **2013**, *12*, 347–357. [CrossRef] [PubMed]
47. Andreu, Z.; Yanez-Mo, M. Tetraspanins in Extracellular Vesicle Formation and Function. *Front. Immunol.* **2014**, *5*, 442. [CrossRef] [PubMed]
48. Liang, X.; Gupta, D.; Xie, J.; Van Wonterghem, E.; Van Hoecke, L.; Hean, J.; Niu, Z.; Ghaeidamini, M.; Wiklander, O.P.B.; Zheng, W.; et al. Engineering of extracellular vesicles for efficient intracellular delivery of multimodal therapeutics including genome editors. *Nat. Commun.* **2025**, *16*, 4028. [CrossRef]
49. Goo, J.; Lee, Y.; Lee, J.; Kim, I.S.; Jeong, C. Extracellular Vesicles in Therapeutics: A Comprehensive Review on Applications, Challenges, and Clinical Progress. *Pharmaceutics* **2024**, *16*, 311. [CrossRef] [PubMed]
50. Alqurashi, H.; Alsharief, M.; Perciato, M.L.; Raven, B.; Ren, K.; Lambert, D.W. Message in a bubble: The translational potential of extracellular vesicles. *J. Physiol.* **2023**, *601*, 4895–4905. [CrossRef]
51. Di Ianni, E.; Obuchi, W.; Breyne, K.; Breakefield, X.O. Extracellular vesicles for the delivery of gene therapy. *Nat. Rev. Bioeng.* **2025**, *3*, 360–373. [CrossRef] [PubMed]
52. Van Delen, M.; Derdelinckx, J.; Wouters, K.; Nelissen, I.; Cools, N. A systematic review and meta-analysis of clinical trials assessing safety and efficacy of human extracellular vesicle-based therapy. *J. Extracell. Vesicles* **2024**, *13*, e12458. [CrossRef] [PubMed]
53. Kondo, Y.; Oubridge, C.; van Roon, A.M.M.; Nagai, K. Crystal structure of human U1 snRNP, a small nuclear ribonucleoprotein particle, reveals the mechanism of 5′ splice site recognition. *eLife* **2015**, *4*, e04986. [CrossRef] [PubMed]
54. Torrisi, S.A.; Geraci, F.; Diolosà, L.; De Luca, A.; Falzone, L.; Drago, F.; Libra, M.; Leggio, G.M. RNA-based drugs: Current, imminent and possible therapeutic applications. *Pharmacol. Ther.* **2026**, *277*, 108958. [CrossRef]
55. Gaspar, A.; Garrido, J.M. Unveiling RNA ligands: Harnessing NMR for hit generation. *Eur. J. Med. Chem.* **2026**, *304*, 118495. [CrossRef]
56. Villarroya-Beltri, C.; Gutiérrez-Vázquez, C.; Sánchez-Cabo, F.; Pérez-Hernández, D.; Vázquez, J.; Martin-Cofreces, N.; Martinez-Herrera, D.J.; Pascual-Montano, A.; Mittelbrunn, M.; Sánchez-Madrid, F. Sumoylated hnRNPA2B1 controls the sorting of miRNAs into exosomes through binding to specific motifs. *Nat. Commun.* **2013**, *4*, 2980. [CrossRef]
57. Santangelo, L.; Giurato, G.; Cicchini, C.; Montaldo, C.; Mancone, C.; Tarallo, R.; Battistelli, C.; Alonzi, T.; Weisz, A.; Tripodi, M. The RNA-Binding Protein SYNCRIP Is a Component of the Hepatocyte Exosomal Machinery Controlling MicroRNA Sorting. *Cell Rep.* **2016**, *17*, 799–808. [CrossRef]
58. Geng, G.; Xu, Y.; Hu, Z.; Wang, H.; Chen, X.; Yuan, W.; Shu, Y. Viral and non-viral vectors in gene therapy: Current state and clinical perspectives. *eBioMedicine* **2025**, *118*, 105834. [CrossRef]
59. Volodina, O.; Smirnikhina, S. The Future of Gene Therapy: A Review of In Vivo and Ex Vivo Delivery Methods for Genome Editing-Based Therapies. *Mol. Biotechnol.* **2025**, *67*, 425–437. [CrossRef]
60. Cecchin, R.; Troyer, Z.; Witwer, K.; Morris, K.V. Extracellular vesicles: The next generation in gene therapy delivery. *Mol. Ther.* **2023**, *31*, 1225–1230. [CrossRef]
61. Kojima, R.; Bojar, D.; Rizzi, G.; Hamri, G.C.E.; El-Baba, M.D.; Saxena, P.; Ausländer, S.; Tan, K.R.; Fussenegger, M. Designer exosomes produced by implanted cells intracerebrally deliver therapeutic cargo for Parkinson's disease treatment. *Nat. Commun.* **2018**, *9*, 1305. [CrossRef] [PubMed]
62. Mulcahy, L.A.; Pink, R.C.; Carter, D.R.F. Routes and mechanisms of extracellular vesicle uptake. *J. Extracell. Vesicles* **2014**, *3*, 24641. [CrossRef]
63. Matera, A.G.; Wang, Z. A day in the life of the spliceosome. *Nat. Rev. Mol. Cell Biol.* **2014**, *15*, 108–121. [CrossRef] [PubMed]
64. Joshi, B.S.; de Beer, M.A.; Giepmans, B.N.G.; Zuhorn, I.S. Endocytosis of Extracellular Vesicles and Release of Their Cargo from Endosomes. *ACS Nano* **2020**, *14*, 4444–4455. [CrossRef] [PubMed]
65. Lai, C.P.; Kim, E.Y.; Badr, C.E.; Weissleder, R.; Mempel, T.R.; Tannous, B.A.; Breakefield, X.O. Visualization and tracking of tumour extracellular vesicle delivery and RNA translation using multiplexed reporters. *Nat. Commun.* **2015**, *6*, 7029. [CrossRef] [PubMed]
66. Wang, S.; Weissman, D.; Dong, Y. RNA chemistry and therapeutics. *Nat. Rev. Drug Discov.* **2025**, *24*, 828–851. [CrossRef]

67. Balestra, D.; Faella, A.; Margaritis, P.; Cavallari, N.; Pagani, F.; Bernardi, F.; Arruda, V.; Pinotti, M. An engineered U1 small nuclear RNA rescues splicing-defective coagulation F7 gene expression in mice. *J. Thromb. Haemost.* **2014**, *12*, 177–185. [CrossRef]
68. Dong, X.; Huang, Y.; Yi, T.; Hu, C.; Gao, Q.; Chen, Y.; Zhang, J.; Chen, J.; Liu, L.; Meng, R.; et al. Intrapleural infusion of tumor cell-derived microparticles packaging methotrexate or saline combined with pemetrexed-cisplatin chemotherapy for the treatment of malignant pleural effusion in advanced non-squamous non-small cell lung cancer: A double-blind, randomized, placebo-controlled study. *Front. Immunol.* **2022**, *13*, 1002938. [CrossRef]
69. Zhu, Y.G.; Shi, M.M.; Monsel, A.; Dai, C.X.; Dong, X.; Shen, H.; Li, S.K.; Chang, J.; Xu, C.L.; Li, P.; et al. Nebulized exosomes derived from allogenic adipose tissue mesenchymal stromal cells in patients with severe COVID-19: A pilot study. *Stem Cell Res. Ther.* **2022**, *13*, 220. [CrossRef]
70. Shapira, S.; Ben Shimon, M.; Hay-Levi, M.; Shenberg, G.; Choshen, G.; Bannon, L.; Tepper, M.; Kazanov, D.; Seni, J.; Lev-Ari, S.; et al. A novel platform for attenuating immune hyperactivity using EXO-CD24 in COVID-19 and beyond. *EMBO Mol. Med.* **2022**, *14*, e15997. [CrossRef]
71. Chiriboga, C.A.; Swoboda, K.J.; Darras, B.T.; Iannaccone, S.T.; Montes, J.; De Vivo, D.C.; Norris, D.A.; Bennett, C.F.; Bishop, K.M. Results from a phase 1 study of nusinersen in children with spinal muscular atrophy. *Neurology* **2016**, *86*, 890–897. [CrossRef]
72. Rietz, A.; Hodgetts, K.J.; Lusic, H.; Quist, K.M.; Osman, E.Y.; Lorson, C.L.; Androphy, E.J. Short-duration splice promoting compound enables a tunable mouse model of spinal muscular atrophy. *Life Sci. Alliance* **2021**, *4*, e202000889. [CrossRef]
73. Calucho, M.; Bernal, S.; Alías, L.; March, F.; Venceslá, A.; Rodríguez-Álvarez, F.J.; Aller, E.; Fernández, R.M.; Borrego, S.; Millán, J.M.; et al. Correlation between SMA type and SMN2 copy number revisited: An analysis of 625 unrelated Spanish patients and a compilation of 2834 reported cases. *Neuromuscul. Disord.* **2018**, *28*, 208–215. [CrossRef]
74. Cao, A.; Galanello, R.; Rosatelli, M. Genotype-phenotype correlations in β-thalassemias. *Blood Rev.* **1994**, *8*, 1–12. [CrossRef]
75. Yim, N.; Ryu, S.W.; Choi, K.; Lee, K.R.; Lee, S.; Choi, H.; Kim, J.; Shaker, M.R.; Sun, W.; Park, J.H.; et al. Exosome engineering for efficient intracellular delivery of soluble proteins using optically reversible protein–protein interaction module. *Nat. Commun.* **2016**, *7*, 12277. [CrossRef]
76. Nechay, M.; Kleiner, R.E. High-throughput approaches to profile RNA-protein interactions. *Curr. Opin. Chem. Biol.* **2020**, *54*, 37–44. [CrossRef] [PubMed]
77. Guo, A.; Cao, Q.; Fang, H.; Tian, H. Recent advances and challenges of injectable hydrogels in drug delivery. *J. Control. Release* **2025**, *385*, 114021. [CrossRef] [PubMed]
78. Liu, B.; Chen, K. Advances in Hydrogel-Based Drug Delivery Systems. *Gels* **2024**, *10*, 262. [CrossRef] [PubMed]
79. Alvarez-Erviti, L.; Seow, Y.; Yin, H.; Betts, C.; Lakhal, S.; Wood, M.J.A. Delivery of siRNA to the mouse brain by systemic injection of targeted exosomes. *Nat. Biotechnol.* **2011**, *29*, 341–345. [CrossRef]
80. Morales-Kastresana, A.; Musich, T.A.; Welsh, J.A.; Telford, W.; Demberg, T.; Wood, J.C.S.; Bigos, M.; Ross, C.D.; Kachynski, A.; Dean, A.; et al. High-fidelity detection and sorting of nanoscale vesicles in viral disease and cancer. *J. Extracell. Vesicles* **2019**, *8*, 1597603. [CrossRef]
81. Obuchi, W.; Zargani-Piccardi, A.; Leandro, K.; Rufino-Ramos, D.; Di Lanni, E.; Frederick, D.M.; Maalouf, K.; Nieland, L.; Xiao, T.; Repiton, P.; et al. Engineering of CD63 Enables Selective Extracellular Vesicle Cargo Loading and Enhanced Payload Delivery. *J. Extracell. Vesicles* **2025**, *14*, e70094. [CrossRef] [PubMed]
82. Han, C.; Yang, J.; Yin, T.; An, J.; Qiao, A.; Cao, Y.; Feng, Y.; Lu, H.; Wang, Y.; Yang, L.; et al. CD63-snorkel tagging for isolation of exosomes. *Extracell. Vesicle* **2023**, *2*, 100031. [CrossRef] [PubMed]

Disclaimer/Publisher's Note: The statements, opinions and data contained in all publications are solely those of the individual author(s) and contributor(s) and not of MDPI and/or the editor(s). MDPI and/or the editor(s) disclaim responsibility for any injury to people or property resulting from any ideas, methods, instructions or products referred to in the content.